



Molecular Crystals and Liquid Crystals

Publication details, including instructions for authors and subscription information:

<http://www.tandfonline.com/loi/gmcl20>

Low Surface Energy Properties of Smectic Fluorinated Block Copolymer/SEBS Blends

Elisa Martinelli ^a, Chiara Fantoni ^a, Giancarlo Galli ^a
, Bernard Gallot ^b & Antonella Glisenti ^c

^a Dipartimento di Chimica e Chimica Industriale,
UdR Pisa INSTM, Università di Pisa, via Risorgimento,
Pisa, Italy

^b Laboratoire des Matériaux Organiques à Propriétés
Spécifiques, CNRS, Vernaison, France

^c Dipartimento di Scienze Chimiche, Università di
Padova, Padova, Italy

Version of record first published: 18 Mar 2009

To cite this article: Elisa Martinelli, Chiara Fantoni, Giancarlo Galli, Bernard Gallot & Antonella Glisenti (2009): Low Surface Energy Properties of Smectic Fluorinated Block Copolymer/SEBS Blends, *Molecular Crystals and Liquid Crystals*, 500:1, 51-62

To link to this article: <http://dx.doi.org/10.1080/15421400802713686>

PLEASE SCROLL DOWN FOR ARTICLE

Full terms and conditions of use: <http://www.tandfonline.com/page/terms-and-conditions>

This article may be used for research, teaching, and private study purposes.
Any substantial or systematic reproduction, redistribution, reselling, loan,

sub-licensing, systematic supply, or distribution in any form to anyone is expressly forbidden.

The publisher does not give any warranty express or implied or make any representation that the contents will be complete or accurate or up to date. The accuracy of any instructions, formulae, and drug doses should be independently verified with primary sources. The publisher shall not be liable for any loss, actions, claims, proceedings, demand, or costs or damages whatsoever or howsoever caused arising directly or indirectly in connection with or arising out of the use of this material.

Low Surface Energy Properties of Smectic Fluorinated Block Copolymer/SEBS Blends

Elisa Martinelli¹, Chiara Fantoni¹, Giancarlo Galli¹,
Bernard Gallot², and Antonella Glisenti³

¹Dipartimento di Chimica e Chimica Industriale, Udr Pisa INSTM,
Università di Pisa, via Risorgimento, Pisa, Italy

²Laboratoire des Matériaux Organiques à Propriétés Spécifiques, CNRS,
Vernaison, France

³Dipartimento di Scienze Chimiche, Università di Padova, Padova, Italy

A smectic polystyrene–poly(perfluorooctylethyl acrylate) block copolymer was synthesized by atom transfer radical polymerization and blended with a thermoplastic elastomer SEBS in different compositions. The mesophase structure and transition temperatures were investigated by DSC and WAXD. Thin films of the block copolymer and the blends exhibited large contact angles with both water and n-hexadecane, which resulted in low solid surface tensions. XPS findings at different photoemission angles confirmed the effective surface segregation of the mesogenic chains of the fluorinated polymer block.

Keywords: block copolymer; fluorinated polymer; mesophase; polymer blend; surface segregation

INTRODUCTION

Block copolymers with mesogenic side chains are able to self-organize on different length scales. Their microstructure is in fact formed under the influence of the two driving forces of microphase separation of the blocks and liquid crystalline ordering of the mesogens [1]. One special

The work was funded by the EC Framework 6 Integrated Project ‘AMBIO’ (Advanced Nanostructured Surfaces for the Control of Biofouling). This article reflects only the authors’ views and the European Commission is not liable for any use that may be made of information contained therein.

Address correspondence to Giancarlo Galli, Dipartimento di Chimica e Chimica Industriale, Udr Pisa INSTM, Università di Pisa, via Risorgimento 35, 56126 Pisa, Italy. E-mail: gallig@cci.unipi.it

case is that of block copolymers carrying perfluorinated side chain mesogens. Pendent perfluoroalkyl groups to a polymer backbone can form smectic-like structures at the surface of thin films, which is mediated by the bulk mesophase order [2–4]. Therefore, an additional structuring effect originates from surface segregation to minimize surface and interface tensions at the solid–air interface. The wettability of fluorinated polymers is markedly influenced by their packing order, and liquid crystalline polymers generally present lower surface tensions than amorphous polymers [5–11]. Because of the inherent non-stick behavior fluorinated polymers are candidates as lubricant, wear control, antisoiling and anti(bio)fouling materials.

Our interest is in developing a low surface energy, low elastic modulus material potentially applicable in fouling release coatings in the marine environment [12]. In this work we incorporated a smectic poly(styrene-*b*-2-perfluorooctylethyl acrylate) diblock copolymer into blends with a commercial thermoplastic elastomer SEBS. Films of such fluorinated block copolymers self-aggregate in hierarchical structures and exhibit a surface mostly covered with perfluoroalkyl groups owing to their low surface energy [13,14]. We highlight the role of the perfluorinated chains of the block copolymer in affecting the bulk and surface properties of the SEBS blends.

EXPERIMENTAL PART

Materials

Trifluorotoluene (TFT), hexafluorobenzene, 2,2'-bipyridine (Bipy), CuBr, 1-phenylethyl bromide (1-(PE)Br) and monomer 2-perfluorooctylethyl acrylate (AF8) (Aldrich) were used without further purification. Styrene (S) (Fluka) was washed with 5% NaOH and water, dried over Na₂SO₄ and distilled under reduced pressure. α,α' -Azobis(isobutyronitrile) (AIBN) (Fluka) was recrystallized from methanol. Polystyrene-*b*-poly(ethylene-*co*-butylene)-*b*-polystyrene (SEBS) triblock elastomer (Kraton G1652M) was kindly provided by Kraton Polymers. The styrene content of SEBS was ~30 wt%.

Styrene–AF8 Random Copolymer

A solution of 3.54 mL (30.94 mmol) of S, 50 mg (0.30 mmol) of AIBN, 4.892 g (3.44 mmol) of AF8 and 15 mL of TFT was degassed by four freeze-thaw pump cycles. The polymerization was let to proceed for 48 h at 65°C, and the polymer was then purified by repeated

precipitations from TFT solutions in methanol (yield 73%). The resulting random copolymer, containing 12 mol% AF8, is denoted by (S-co-AF8).

^1H NMR (CDCl_3): δ (ppm) = 0.4–2.8 (27.85H, CH_2CH , CH_2CF_2), 3.0–4.2 (2.00H, COOCH_2), 5.6–8.0 (38.09H, aromatic).

^{19}F NMR ($\text{CDCl}_3/\text{hexafluorobenzene}$): δ (ppm) = 36 (2.0 F, CF_2), 38–41 (10.1 F, CF_2), 48 (2.0 F, CF_2CH_2), 81 (3.0 F, CF_3).

FT-IR (film): $\bar{\nu}$ (cm^{-1}) = 3150–2990 (ν C–H aromatic), 2990–2825 (ν C–H aliphatic), 1740 (ν C=O), 1603 (ν C=C aromatic), 1495 and 1455 (δ C–H aliphatic), 1400–1000 (ν C–O and ν C–F), 761 and 701 (δ C–H aromatic), 656 (ω CF_2).

Polystyrene–AF8 Block Copolymer

In a first step, a solution of 20.00 mL (174.81 mmol) of S, 1.022 g (6.54 mmol) of Bipy, and 0.30 mL (2.18 mmol) of 1-(PE)Br was purged with nitrogen for 15 min and then 0.313 g (2.18 mmol) of CuBr was added. After four freeze-thaw pump cycles, the polymerization was let to proceed for 330 min at 110°C. After cooling to room temperature, the polymer solution was diluted with THF and then eluted on neutral alumina. The polymer was purified by repeated precipitations from THF solutions in methanol (yield 85%). The resulting Br-terminated polystyrene macroinitiator (average degree of polymerization, $n = 58$) is denoted by P(S).

In a second step, 1.11 g (0.18 mmol) of P(S) and 85.0 mg (0.54 mmol) of Bipy were flushed with nitrogen three times. A solution of 1.890 g (3.65 mmol) of AF8 in 11 mL of TFT was added under nitrogen. After four freeze-thaw pump cycles, 27.1 mg (0.19 mmol) of CuBr was added and the solution was subjected to four freeze-thaw pump cycles. The polymerization was let to proceed for 86 h at 115°C. When the reaction was stopped the polymer solution was diluted with TFT and washed with water until the disappearance of greenish color. The solvent was removed under vacuum and the polymer was precipitated from TFT solution in methanol (yield 51%). The resulting diblock copolymer, containing 9 mol% AF8 (average degree of polymerization, $m = 6$), is denoted by (S-*b*-AF8).

^1H NMR (CDCl_3): δ (ppm) = 1.2–2.8 (34.98H, CH_2CH , CH_2CF_2), 4.5 (2.00H, COOCH_2), 6.2–7.4 (49.97H aromatic).

^{19}F NMR ($\text{CDCl}_3/\text{hexafluorobenzene}$): δ (ppm) = 36 (2.0 F, CF_2), 38–41 (10.0 F, CF_2), 48 (2.0 F, CF_2CH_2), 81 (3.1 F, CF_3).

FT-IR (film): $\bar{\nu}$ (cm^{-1}) = 3150–3990 (ν C–H aromatic), 2990–2800 (ν C–H aliphatic), 1739 (ν C=O), 1602 (ν C=C aromatic), 1494 and

1453 (δ C–H aliphatic), 1400–1000 (ν C–O and ν C–F), 757 and 699 (δ C–H aromatic), 658 (ω CF₂).

Polymer Blends

Blends were prepared by co-precipitation of a 1 wt% chloroform solution of block copolymer (S-*b*-AF8) and SEBS in methanol. They are denoted as (S-*b*-AF8)X, where X is the wt% of block copolymer (X = 10–90).

Film Deposition

The polymer films were obtained by spin coating 3 wt% TFT solutions of the polymer alone or blended with SEBS (10–90 wt%) on glass slides. They were vacuum dried overnight and then annealed at 120°C for 15 h (thickness 200–400 nm).

Characterization

¹H (vs. TMS) and ¹⁹F (vs. hexafluorobenzene) spectra were recorded on Varian Gemini VRX 200 and Varian Gemini VRX 300 spectrometers, respectively.

Number (M_n) and weight (M_w) average molecular weights and polydispersities (M_w/M_n) were measured by size exclusion chromatography (SEC) using a Jasco PU-1580 liquid chromatograph equipped with two PL gel 5 μ m Mixed-D columns, a Jasco 830-RI refractive index detector and a Perkin-Elmer LC75 UV detector. Polystyrene standards ($4.0 \cdot 10^2$ – $4.0 \cdot 10^5$ g/mol) were used for calibration.

Differential scanning calorimetry (DSC) measurements were performed with a Mettler DSC-30 instrument (10°C/min). The phase transition temperatures were taken at the maximum temperature in the DSC enthalpic peaks of the second heating cycles. The glass transition temperature (T_g) was set at the half-devitrification temperature.

Wide angle X-ray diffraction (WAXD) patterns were recorded with a home made diffractometer equipped with a flat film camera. The Ni-filtered CuK α radiation was used ($\lambda = 1.54$ Å). Polymer powder samples were studied from room temperature up to the isotropization temperature.

Static contact angle measurements were carried out with a FTA200 Camtel goniometer using as interrogating liquids water, *n*-hexadecane and ethylene glycol of the highest purity commercially available (>99%).

X-ray photoelectron spectroscopy (XPS) spectra were recorded with a Perkin-Elmer PHI 5600 spectrometer with a standard Al-K α source (1486.6 eV) operating at 350 W. The working pressure was less than 10^{-8} Pa. The spectrometer was calibrated by assuming the binding energy (BE) of the Au 4f $_{7/2}$ line to be 84.0 eV with respect to the Fermi level. Extended spectra (survey) were collected in the range 0–1350 eV (187.85 eV pass energy, 0.5 eV step, 0.025 s/step). Detailed spectra were recorded for the C (1 s), O (1 s), and F (1 s) regions (11.75 eV pass energy, 0.1 eV step, 0.1 s/step). The standard deviation in the BE values of the XPS line was 0.10 eV. The atomic percentage, after a Shirley type background subtraction [15], was evaluated using the PHI sensitivity factors [16]. To take into account charging problems, the hydrocarbon peak was adjusted to a position of 285.0 eV and the sub-peak BE differences were evaluated.

RESULTS AND DISCUSSION

Synthesis

The diblock copolymer (S-*b*-AF8) was prepared by a two-step procedure based on two successive atom transfer radical polymerizations (ATRP) (Fig. 1).

In the first step, a bromo-terminated polystyrene macroinitiator P(S) ($M_n = 6.1 \cdot 10^3$ g/mol, $n = 58$) was prepared by ATRP of styrene, S, in bulk with 1-phenylethyl bromide as an initiator and CuBr/2,2'-bipyridine as a catalyst (1:1:3 molar ratio) at 110°C. In the second step, the copolymerization for attachment of the block of fluorinated acrylate monomer AF8 to the polystyrene block was carried out in TFT solution at 115°C. The length of the AF8 block ($m = 6$; 9 mol%) was calculated from the known length of the S block. The SEC elution curves were monomodal with a narrow polydispersity ($M_w/M_n = 1.21$), indicating that the polymerizations proceeded under a controlled mechanism without significant deactivation of the propagating polymer species. Therefore, by taking advantage of the capability of ATRP a block copolymer was devised in which the AF8 content was low

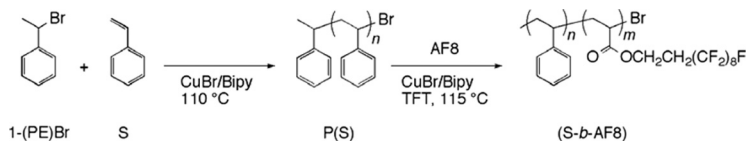


FIGURE 1 Synthesis of block copolymer (S-*b*-AF8) by ATRP.

enough to enable easy processing and blending. A random copolymer (S-*co*-AF8) (12 mol% AF8) was prepared by conventional free radical polymerization initiated by AIBN in TBT at 65°C and taken as a reference compound for the block copolymer.

The fluorinated block copolymer was used as a surface active component to prepare blends (S-*b*-AF8)*X* with the thermoplastic elastomer SEBS in varied proportions (*X* = 10–90 wt% block copolymer). The blends were formulated so as to tune the elastic modulus and surface energy of the films, in order to develop a general methodology for creating novel coatings potentially capable of inhibiting the adhesion and/or promoting the release of marine micro- and macro-organisms.

Thermal and Mesophase Behavior

The thermal properties of the block copolymer and the SEBS blends were studied by DSC, with particular attention to detection of thermotropic mesophases and their phase transitions.

The block copolymer (S-*b*-AF8) exhibited a clear transition peak at 71°C ($\Delta H_i = 0.9$ J/g), associated with the isotropization of a mesophase of the fluorinated block, and a glass transition at 93°C due to the polystyrene block. The liquid crystal behavior was confirmed by WAXD studies. The diffraction patterns displayed up to three small-angle Bragg reflections indicative of a correlated layered structure (periodicity 32.6 Å), in which the fluorocarbon chains were arranged on a pseudo-hexagonal lattice (side of the hexagon $a_H = 5.9$ Å) and tilted with respect to the layer normal by an angle of 16° (SmI₂ or SmF₂ mesophase) (Fig. 2). By contrast, no evidence of mesophase formation was detected for the random copolymer either by DSC or X-ray diffraction studies. Whereas in (S-*b*-AF8) each block preserved the glass and

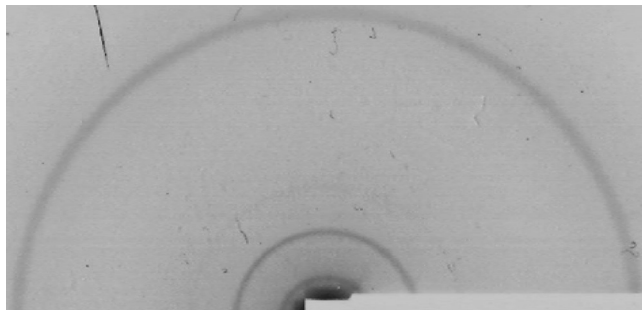


FIGURE 2 WAXD pattern of the smectic mesophase of (S-*b*-AF8) at 25°C.

TABLE 1 Thermal Transitions of Copolymers and Blends with SEBS

Sample	SEBS (wt%)	T_g^a (°C)	T_m^a (°C)	T_i^b (°C)	T_g^c (°C)
(S- <i>co</i> -AF8)	0			—	73
(S- <i>b</i> -AF8)	0			71	93
(S- <i>b</i> -AF8)90	10	—	—	72	93
(S- <i>b</i> -AF8)70	30	—	17	72	94
(S- <i>b</i> -AF8)50	50	−56	18	73	93
(S- <i>b</i> -AF8)30	70	−55	17	74	95
(S- <i>b</i> -AF8)10	90	−53	17	—	—
SEBS	100	−59	17		

^aGlass transition and melting temperatures of the ethylene-*co*-butylene block of SEBS.

^bIsotropization temperature of the fluorinated block of the block copolymer.

^cGlass transition temperature of the polystyrene block of the block copolymer.

mesophase behavior of their respective homopolymers, the incorporation of an almost same amount of non-mesogenic counits in a statistical manner into (S-*co*-AF8) introduced constitutional irregularity which did not permit the onset of liquid crystalline order. The phase transition temperatures of the blends are collected in Table 1 and compared with those of SEBS and the copolymers.

SEBS presented a glass transition at −59°C and a melting transition at 17°C due to the partially crystalline ethylene-*co*-butylene block. The T_g of the polystyrene block was not detected because of its low content in the triblock copolymer. The blend (S-*b*-AF8)10, richer in SEBS, exhibited all the transitions typical of SEBS only. Conversely, the blend (S-*b*-AF8)90, poorer in SEBS, presented all the thermal transitions of the block copolymer only. The DSC traces of the blends with intermediate SEBS contents resulted from the superimposition of the SEBS and block copolymer curves, with the relative intensities of the transitions depending on the blend composition (Table 1). These results suggest that the blend components were chemically incompatible and segregated in different (micro)phases. We assume that the block copolymer was selectively located at the interface with SEBS and/or within the SEBS polystyrene domains, thus originating a supra-molecular structure.

Wetting Behavior and Surface Energy

The wetting behavior of the copolymers and the blends was studied by measurements of the static contact angle θ of thin films (200–400 nm thickness) using water, ethylene glycol and *n*-hexadecane as wetting

TABLE 2 Static Contact Angles^a and Surface Tensions^b of Copolymers and Blends With SEBS

Film	θ_w (°)	θ_h (°)	θ_{EG} (°)	γ_S^{OWKb} (mN/m)	γ_S^{db} (mN/m)	γ_S^{pb} (mN/m)
(S-co-AF8)	109 ± 1	58 ± 1	94 ± 1	16.8	16.1	0.7
(S-b-AF8)	120 ± 1	80 ± 1	101 ± 1	9.7	9.4	0.3
(S-b-AF8)90	119 ± 1	81 ± 1	101 ± 1	9.7	9.3	0.4
(S-b-AF8)70	119 ± 1	80 ± 1	100 ± 1	9.7	9.3	0.4
(S-b-AF8)50	118 ± 1	82 ± 1	101 ± 1	9.5	9.0	0.5
(S-b-AF8)30	118 ± 1	80 ± 1	100 ± 1	10.0	9.5	0.5
(S-b-AF8)10	108 ± 2	59 ± 1	97 ± 1	16.8	15.7	0.9

^aContact angles measured with water, *n*-hexadecane, and ethylene glycol.

^bCalculated with the Owens–Wendt–Kaelble method: γ_S^d dispersion component, γ_S^p polar component.

liquids (Table 2). The films were spin-coated onto glass slides, dried under vacuum overnight and then annealed for 15 h at 120°C to achieve equilibrium morphologies.

The values of θ with water and *n*-hexadecane are conventionally used to estimate qualitatively hydrophobicity ($\theta_w > \sim 90^\circ$) and lipophobicity ($\theta_h > \sim 60^\circ$) of a polymer film, respectively. The block copolymer showed high static contact angles with all the interrogating liquids, exhibiting in particular strong hydrophobic ($\theta_w = 120^\circ$) and lipophobic ($\theta_h = 80^\circ$) properties. This two-fold character is typical of fluorinated polymers, as opposed to other polymers, namely polyolefins, that are hydrophobic, but not lipophobic at the same time. Both θ_w and θ_h for the block copolymer were much larger than for the random copolymer, but essentially equal to those for most of the blends. The latter were unaffected by the blend composition, even at contents of SEBS as high as 70 wt%. It appears that the statistical distribution of the fluorinated units in the random copolymer results in a less effective segregation of the pendant fluorinated chains at the solid–air interface. On the other hand, the chemical incompatibility between the fluorinated block copolymer and SEBS enhances the self-assembly of the fluorinated chains at the outer surface of the films and induces distinct non-wetting properties. The phenomenon of surface segregation is known for a variety of fluorinated polymers [17,18], polymer blends and networks [19–21] and is here pursued as a tool to construct low surface energy, low adhesion polymer coatings.

Measurements of liquid–solid contact angles are commonly used to evaluate solid surface tension γ_S . However, the correlation between θ and γ is still a controversial question and none of the different

approaches proposed are generally accepted [22,23]. Accordingly, we followed the additive-component methods of the surface tension of Owens, Wendt, and Kaelble (OWK) [24,25] and van Oss, Chaudhury, and Good [26,27], by using different wetting liquids of known surface tension γ_L . As the γ_S values calculated with the two different methods were in excellent agreement with each other, we report on the OWK method only (γ_S^{OWK}). In this approach the solid surface tension:

$$\gamma_S = \gamma_S^d + \gamma_S^p \quad (1)$$

combined with the Young's equation yields:

$$\gamma_L(1 + \cos \theta) = 2[(\gamma_S^d + \gamma_L^d)^{1/2} + (\gamma_S^p + \gamma_L^p)^{1/2}] \quad (2)$$

where γ^d and γ^p are the dispersion and the polar components of surface tension, respectively. Since there are two unknowns (γ_S^d , γ_S^p), it is necessary to use at least two probing liquids of known γ_L^d and γ_L^p . The surface tensions and the related components calculated for the copolymers and the blends are also collected in Table 2.

The values of the γ_S^{OWK} were consistent with a low surface energy of the polymer films, being in the range of 9–17 mN/m. In any case, the dispersive component overwhelmed the associated polar component in determining the total surface tension. This behavior is typical of fluorinated surfaces which experience dispersion forces but prevent polar, e.g., dipole–dipole or hydrogen bonding, interactions. The surface tensions of the blends were similar to that of the block copolymer, and therefore the surface properties were dominated by the fluorinated copolymer. For the blend (S-*b*-AF8)/10 the highest content of SEBS resulted in a comparatively high surface tension.

Surface Analysis

To substantiate better the surface segregation of the fluorinated block we started an analysis of the chemical composition of the film surface by angle-dependent X-ray photoelectron spectroscopy (XPS) measurements. Spectra were recorded at different photoemission angles $\phi = 70^\circ$, 50° , and 20° , that corresponded to increasing sampling depths in the range 3–10 nm.

We focus our attention on the films of the block copolymer and its blend (S-*b*-AF8)/90. The survey spectra of the films demonstrated the presence of no other elements than C, O and F in the range of binding energy up to 800 eV (Fig. 3) [28]. The C(1s) peak revealed a complex shape, and the fitting procedure indicated the presence of

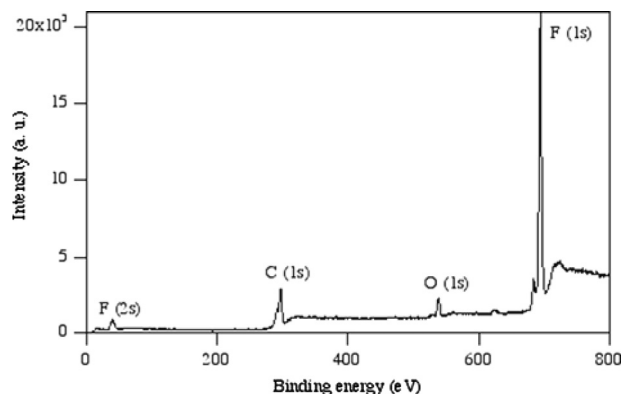


FIGURE 3 XPS survey spectrum at $\phi = 50^\circ$ for (S-b-AF8).

several overlapping contributions. The signals due to the CF_2 and CF_3 moieties were clearly identified at ~ 291 eV and ~ 293 eV, respectively (Fig. 4).

The elemental analysis data for the different angles ϕ are summarized in Table 3, where they are also compared with the corresponding values calculated from the known ‘stoichiometric’ composition of the block copolymer. The atomic percentages slightly changed with angle ϕ , consistent with a composition gradient normal to the film surface into the bulk. For the block copolymer the F atomic percentage was markedly higher (60.1%) than the stoichiometric one (18%) and decreased with decreasing ϕ , whereas the C atomic percentage followed the opposite trend. Thus, the outermost surface of the films was selectively enriched by the low energy fluorinated block. The O atomic percentage was generally comparable with the anticipated

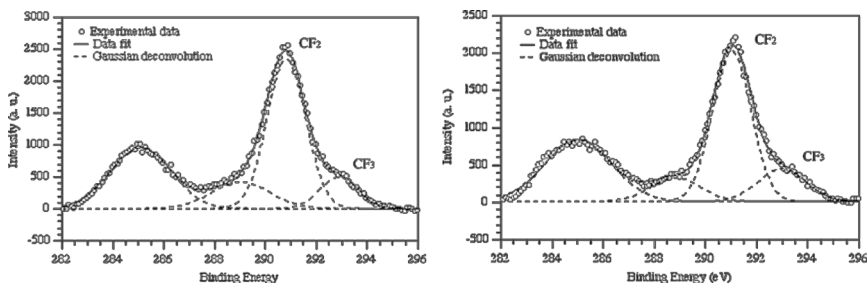


FIGURE 4 C(1s) XPS spectra at $\phi = 50^\circ$ for (S-b-AF8) (left) and (S-b-AF8)90 (right).

TABLE 3 XPS Atomic Composition of (S-*b*-AF8) and a Blend With SEBS

Film	ϕ (°)		C (%)	O (%)	F (%)
(S- <i>b</i> -AF8)		Stoichiometric ^a	80	2	18
	70	Experimental	35.3	4.6	60.1
	50		36.6	5.6	57.8
	20		37.8	5.4	56.8
(S- <i>b</i> -AF8)90					
	70	Experimental	32.8	4.7	62.5
	50		35.4	5.4	59.2
	20		41.6	5.6	52.8

^aCalculated on the basis of the known degrees of polymerization n and m .

nominal composition and slightly increased with increasing sampling depth, according to the increment of the ester group concentration in the underlying molecular layers of the polymer films. This behavior is even more evident in the blend. Even though it is not possible to compare the XPS experimental results with the stoichiometric ones because of the uncertainty of the actual SEBS composition, the detected F atomic percentages are much larger than those we expected for the blend and very close to those detected for the neat block copolymer. A strong surface segregation of the fluorinated tails takes place in the blend, which is possibly enhanced over that of the block copolymer itself.

CONCLUSIONS

Blends of smectic block copolymer (S-*b*-AF8) with SEBS present low wetting properties irrespective of the chemical composition, at least up to 70 wt% SEBS. Such behavior is associated with the segregation of the mesogenic side chains of the fluorinated polymer block to the outer surface. The blend films can combine low surface energy of fluorinated copolymer and low elastic modulus of elastomer SEBS. These two paired features may be expected to provide release properties against marine foulants, such as barnacles, to the polymer films by allowing the adhered organisms to detach from the surface under low shear stresses.

REFERENCES

- [1] de Jeu, W. H., Serero, Y., & Al-Hussein, M. (2005). *Adv. Polym. Sci.*, 181, 75.
- [2] Lüning, J., Stöhr, J., Song, K. Y., Hawker, C. J., Iodice, P., Nguyen, C. V., & Yoon, D. Y. (2001). *Macromolecules*, 34, 1128.

- [3] Al-Hussein, M., Serero, Y., Kononov, O., Mourrano, A., Möller, M., & de Jeu, W. H. (2005). *Macromolecules*, *38*, 9610.
- [4] Busch, P., Krishnan, S., Paik, M., Toombes, G. E. S., Smilgies, D.-M., Gruner, S. M., & Ober, C. K. (2007). *Macromolecules*, *40*, 81.
- [5] Wang, J., Mao, G., Ober, C. K., & Kramer, E. J. (1997). *Macromolecules*, *30*, 1906.
- [6] Krupers, M., Slangen, P.-J., & Möller, M. (1998). *Macromolecules*, *31*, 2558.
- [7] Tsibouklis, J., Graham, P., Eaton, P. J., Smith, J. R., Nevell, T. G., Smart, J. D., & Ewen, R. J. (2000). *Macromolecules*, *33*, 8460.
- [8] Li, X., Andruzzi, L., Chiellini, E., Galli, G., Ober, C. K., Hexemer, A., Kramer, E. J., & Fisher, D. A. (2002). *Macromolecules*, *35*, 8078.
- [9] Granville, A. M., Boyes, S. G., Akgun, B., Foster, M. D., & Brittain, W. J. (2004). *Macromolecules*, *37*, 2790.
- [10] Fujimori, A., Shibasaki, Y., Araki, T., & Nakahara, H. (2004). *Macromol. Chem. Phys.*, *205*, 843.
- [11] Urushihara, Y. & Nishino, T. (2005). *Langmuir*, *21*, 2614.
- [12] Krishnan, S., Weinman, C. J., & Ober, C. K. (2008). *J. Mater. Chem.*, *18*, 3405.
- [13] Hikita, M., Tanaka, K., Nakamura, T., Kajiyama, T., & Takahara, A. (2004). *Langmuir*, *20*, 5304.
- [14] Tanaka, K., Sanada, N., Hikita, M., Nakamura, T., Kajiyama, T., & Takahara, A. (2008). *Appl. Surf. Sci.*, *254*, 5435.
- [15] Shirley, D. A. (1972). *Phys. Rev. B*, *5*, 4709.
- [16] Moulder, J. F., Stickie, W. F., Sobol, P. E., & Bomben, K. D. (1995). *Handbook of X-ray Photoelectron Spectroscopy*. Physical Electronics: Eden Prairie, MN.
- [17] Pospiech, D., Jehnichen, D., Gottwald, A., Häussler, L., Kollig, W., Grundke, K., Janke, A., Schmidt, S., & Werner, C. (2003). *Surf. Coat. Internat., Part B: Coat. Trans.*, *86*, 43.
- [18] Perutz, S., Dai, C.-A., Ober, C. K., & Kramer, E. J. (1996). *Macromolecules*, *29*, 1229.
- [19] Gan, D., Mueller, A., & Wooley, K. L. (2003). *J. Polym. Sci., Part A: Polym. Chem.*, *41*, 3531.
- [20] Gudipati, C. S., Finlay, J. A., Callow, J. A., Callow, M. E., & Wooley, K. L. (2005). *Langmuir*, *21*, 3044.
- [21] Martinelli, E., Agostini, S., Galli, G., Chiellini, E., Glisenti, A., Pettitt, M. E., Callow, M. E., Callow, J. A., Graf, K., & Bartels, F. (2008). *Langmuir*, *24*, 13138.
- [22] Della Volpe, C., Maniglio, D., Brugnara, M., Siboni, S., & Morra, M. (2004). *J. Colloid Interface Sci.*, *271*, 434.
- [23] Siboni, S., Della Volpe, C., Maniglio, D., & Brugnara, M. (2004). *J. Colloid Interface Sci.*, *271*, 454.
- [24] Owens, D. K. & Wendt, R. C. (1969). *J. Appl. Polym. Sci.*, *13*, 1741.
- [25] Kaelble, D. H. (1970). *J. Adhesion*, *2*, 66.
- [26] Good, R. J., Chaudhury, M. K., & van Oss, C. J. (1986). *J. Colloid. Interface Sci.*, *111*, 378.
- [27] Good, R. J., Chaudhury, M. K., & van Oss, C. J. (1988). *Langmuir*, *4*, 884.
- [28] *X-ray Photoelectron Spectroscopy Database* 20, Version 3.0, National Institute of Standards and Technology, Gaithersburg, MD.